Supplemental Materials

Molecular Biology of the Cell

Mathiowetz et al.

SUPPLEMENTAL MATERIAL

TABLE S1. KEY REAGENTS.

REAGENT	SOURCE	CATALOG #
Antibodies and Probes		
Rabbit anti-WHAMM(WT)	Shen et al., 2012	N/A
Chicken anti-WHAMM(WCA)	Campellone et al., 2008	N/A
Guinea Pig anti-WHAMM(CC)	Campellone et al., 2008	N/A
Rabbit anti-MBP	Shen et al., 2012	N/A
Rabbit anti-GFP	Campellone et al., 2008	N/A
Mouse anti-Tubulin	Iowa DHSB	Cat.# E7-C
Mouse anti-ERGIC-53	Alexis Biochemicals	discontinued
Rabbit anti-LC3A	Cell Signaling Technology	Cat.# 4599
Rabbit anti-LC3B	Cell Signaling Technology	Cat.# 3868
Rabbit anti-WDR73	Santa Cruz Biotechnology	Cat.# sc-137933
Mouse anti-GAPDH	Ambion	Cat.# AM4300
Mouse anti-Ubiquitin FK2	Enzo Life Sciences	Cat.# PW8810
Rat anti-GRP94	Novus Biologicals	Cat.# 300-619
Mouse anti-SEC31A	BD Biosciences	Cat.# 612350
Mouse anti-GM130	BD Biosciences	Cat.# 610822
Mouse anti-LAMP1	Santa Cruz Biotechnology	Cat.# sc-18821
Mouse anti-HA.11	Covance	Cat.# 901502
Alexa555 goat anti-mouse IgG	Life Technologies	Cat.# A21424
Alexa555 goat anti-rabbit IgG	Life Technologies	Cat.# A21429
Alexa488 goat anti-rat IgG	Life Technologies	Cat.# A11006
Alexa488 goat anti-guinea pig IgG	Life Technologies	Cat.# A11073
IRDye800CW donkey anti-mouse	LI-COR	Cat.# 926-32212
IRDye800CW donkey anti-rabbit	LI-COR	Cat.# 926-32213

IRDye800CW donkey anti-chicken	LI-COR	Cat.# 926-32218
HRP sheep anti-mouse IgG	GE Healthcare	Cat.# NXA931
HRP donkey anti-rabbit IgG	GE Healthcare	Cat.# NA934V
HRP donkey anti-chicken IgY	Jackson Immunoresearch	Cat.#703035155
Alexa488-Phalloidin	Life Technologies	Cat.# A12379
Alexa647-Phalloidin	Life Technologies	Cat.# A22287
Alexa488-Streptavidin	Life Technologies	Cat.# S32354
Clinical Samples		
Human: Amish Lymphoblastoid Cell Lines (7 patients)	This paper	N/A
Human: Amish Primary Fibroblasts (4 patients)	This paper	N/A
Recombinant Proteins		
MBP-WHAMM(WT) protein	Shen et al., 2012	N/A
MBP-WHAMM(Δ7) protein	This paper	N/A
MBP-WHAMM(X6) protein	This paper	N/A
MBP protein	Shen et al., 2012	N/A
MBP-WHAMM(WMD) protein	Shen et al., 2012	N/A
MBP-WMD(WT) protein (codon optimized)	This paper	N/A
MBP-WMD(RF/AA) protein (codon optimized)	This paper	N/A
GST-Rab1 protein	Russo et al., 2016	N/A
GST protein	Russo et al., 2016	N/A
Cell Lines		
Human: HAP1 cells (mostly haploid parental cell line for eHAP cells)	Haplogen (now Horizon Genomics)	Cat.# C631
Human: eHAP cells (fully haploid parental cell line for WHAMM and WDR73 mutants)	Haplogen; (Essletzbichler et al., 2014)	N/A

Human: WHAMM ^{MUT} eHAP cells (10bp deletion in exon 2)	Haplogen (now Horizon Genomics); This paper	N/A
Human: WDR73 ^{MUT} eHAP cells (10bp insertion in exon 1)	Haplogen (now Horizon Genomics); This paper	N/A
Monkey: Cos7 cells	UC Berkeley Cell Culture Facility	N/A
Human: HeLa cells	UC Berkeley Cell Culture Facility	N/A
Mouse: NIH3T3 cells	UC Berkeley Cell Culture Facility	N/A
Mouse: NIH3T3 cells + LAP vector	This paper	N/A
Mouse: NIH3T3 cells + LAP-WHAMM(WT)	This paper	N/A
Mouse: NIH3T3 cells + LAP-WHAMM(Δ7)	This paper	N/A
Spodoptera: Sf9 cells	Expression Systems, Davis CA	N/A
Recombinant DNA		
pHA vector (pHM6)	Roche	N/A
pHA-WHAMM(WT)	Campellone et al., 2008	N/A
pHA-WHAMM(Δ7)	This paper	N/A
pHA-WHAMM(X6)	This paper	N/A
pKC-LAP-C1 (His-GFP-TEV-S) vector	Campellone et al., 2008	N/A
pKC-LAP-WHAMM(WT)	Campellone et al., 2008	N/A
pKC-LAP-WHAMM(Δ7)	This paper	N/A
pKC-LAP-WHAMM(X6)	This paper	N/A
pKC-mCherry-WHAMM(WT)	Campellone et al., 2008	N/A
pKC-mCherry-WHAMM(X6)	This paper	N/A
pKC-EGFP-C1	Campellone et al., 2008	N/A
pKC-EGFP-WHAMM(WT)	Campellone et al., 2008	N/A
pKC-EGFP-WDR73(WT)	This paper	N/A

pKC-EGFP-WMD(WT) (codon optimized)	This paper	N/A
pKC-EGFP-WMD(RF/AA) (codon optimized)	This paper	N/A
pGFP-DFCP1	Addgene	Cat.# 38269
pKC-FastBac-MBP	Shen et al., 2012	N/A
pKC-FastBac-MBP-WHAMM(WT)	Shen et al., 2012	N/A
pKC-FastBac-MBP-WHAMM(Δ7)	This paper	N/A
pKC-FastBac-MBP-WHAMM(X6)	This paper	N/A
pKC-FastBac-MBP-WHAMM(WMD)	Shen et al., 2012	N/A
pKC-FastBac-GST	Russo et al., 2016	N/A
pKC-FastBac-GST-Rab1	Russo et al., 2016	N/A
pKC-FastBac-MBP-WMD(WT) (codon optimized)	This paper	N/A
pKC-FastBac-MBP-WMD(RF/AA) (codon optimized)	This paper	N/A
Bacmid-MBP	Shen et al., 2012	N/A
Bacmid-MBP-WHAMM(WT)	Shen et al., 2012	N/A
Bacmid-MBP-WHAMM(Δ7)	This paper	N/A
Bacmid-MBP-WHAMM(X6)	This paper	N/A
Bacmid-MBP-WHAMM(WMD)	Shen et al., 2012	N/A
Bacmid-GST	Russo et al., 2016	N/A
Bacmid-GST-Rab1	Russo et al., 2016	N/A
Bacmid-MBP-WMD(WT) (codon optimized)	This paper	N/A
Bacmid-MBP-WMD(RF/AA) (codon optimized)	This paper	N/A
Sequence-Based Reagents		
Human WHAMM (Gene ID: 123720)	N/A	N/A
Human WDR73 (Gene ID: 84942)	N/A	N/A
Negative: siControl	Invitrogen	Cat.# 4390843
Negative: siControl	Invitrogen	Cat.# 12935300

Human/Mouse/Rat: siGAPDH	Invitrogen	Cat.# AM4624
Human: siWHAMM #1	Invitrogen	ID# HSS151263
Human: siWHAMM #2	Invitrogen	ID# HSS151264
Human: siWHAMM #3	Invitrogen	ID# HSS151265
Human: siWDR73 #1	Invitrogen	ID# HSS131519
Human: siWDR73 #2	Invitrogen	ID# HSS189285
Human: siWDR73 #3	Invitrogen	ID# HSS189286

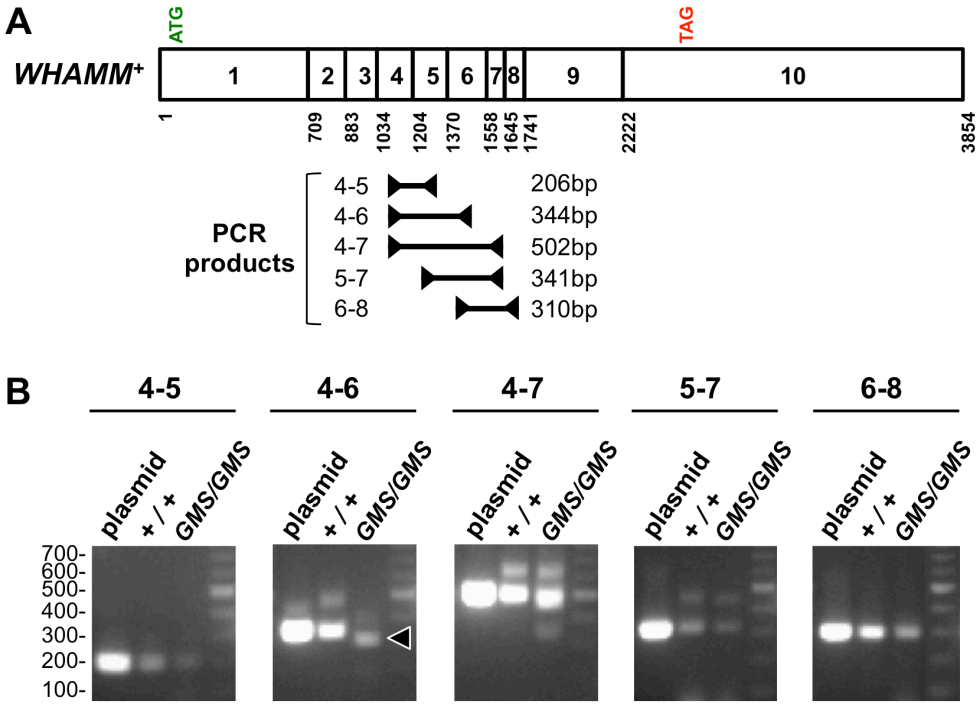

Figure S1. Amish GMS patient fibroblasts express multiple WHAMM mRNA species and predicted proteins.
A. A diagram of the exon organization in wild type *WHAMM* cDNA is shown. The nucleotide numbers at exon junctions are indicated. Start and stop codons are depicted in green and red, respectively. PCR product sizes spanning the indicated exons are also shown in base pairs.
B. RNA was isolated from normal (+/+) or GMS patient (*GMS*/*GMS*) fibroblasts, reverse transcribed, and subjected to PCR with primers specific to the indicated exons of *WHAMM*. A plasmid encoding wild type WHAMM was used as a positive control. The arrowhead highlights the position of a smaller-than-expected product that was amplified using primers in exons 4 and 6. Sequencing revealed that this product contained cryptic exon X6.

C

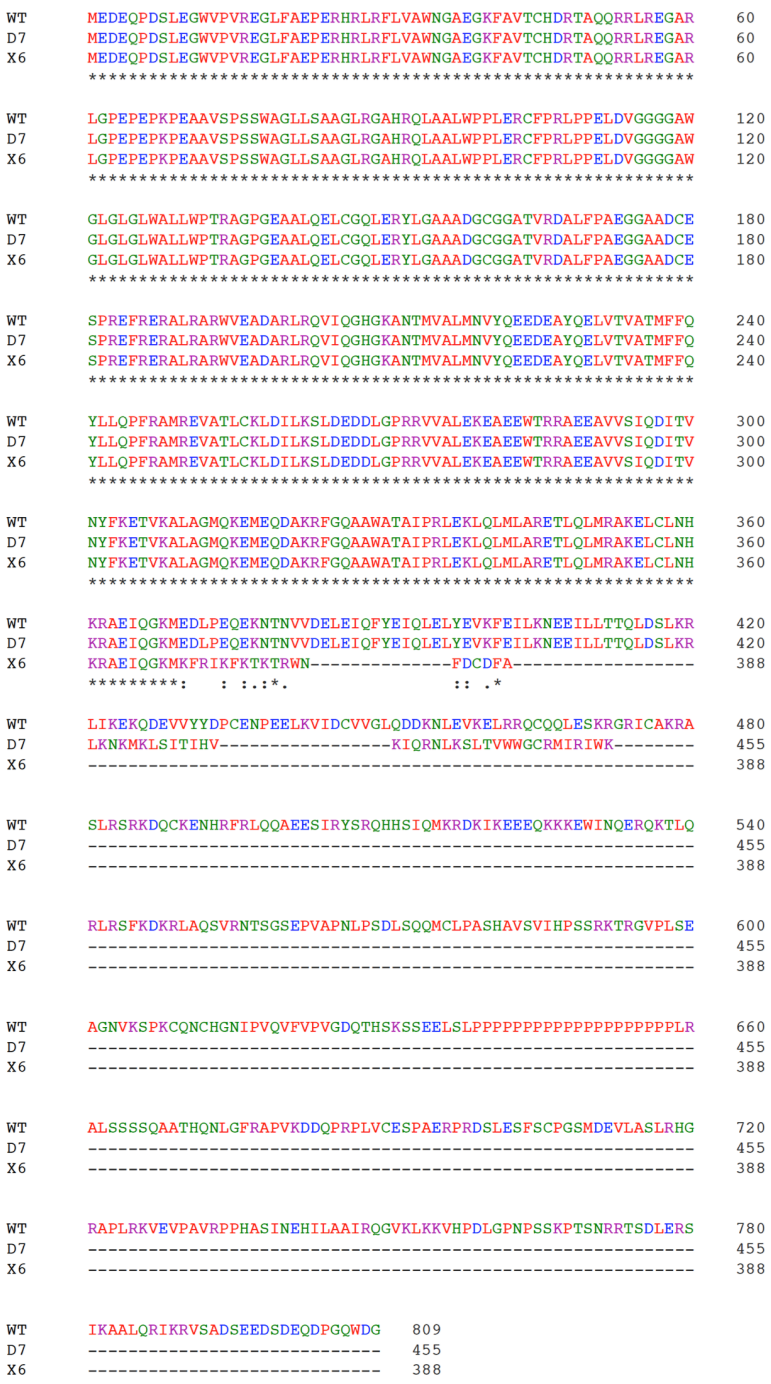

Figure S1 (cont.). Amish GMS patient fibroblasts express multiple WHAMM mRNA species and predicted proteins.
C. A Clustal Omega alignment of the proteins encoded by the *WHAMM*$^{+}$ (“WT”), *WHAMM*^{GMS}*Δ7* (“D7”), and *WHAMM*^{GMS}*X6* (“X6”) transcripts is shown.

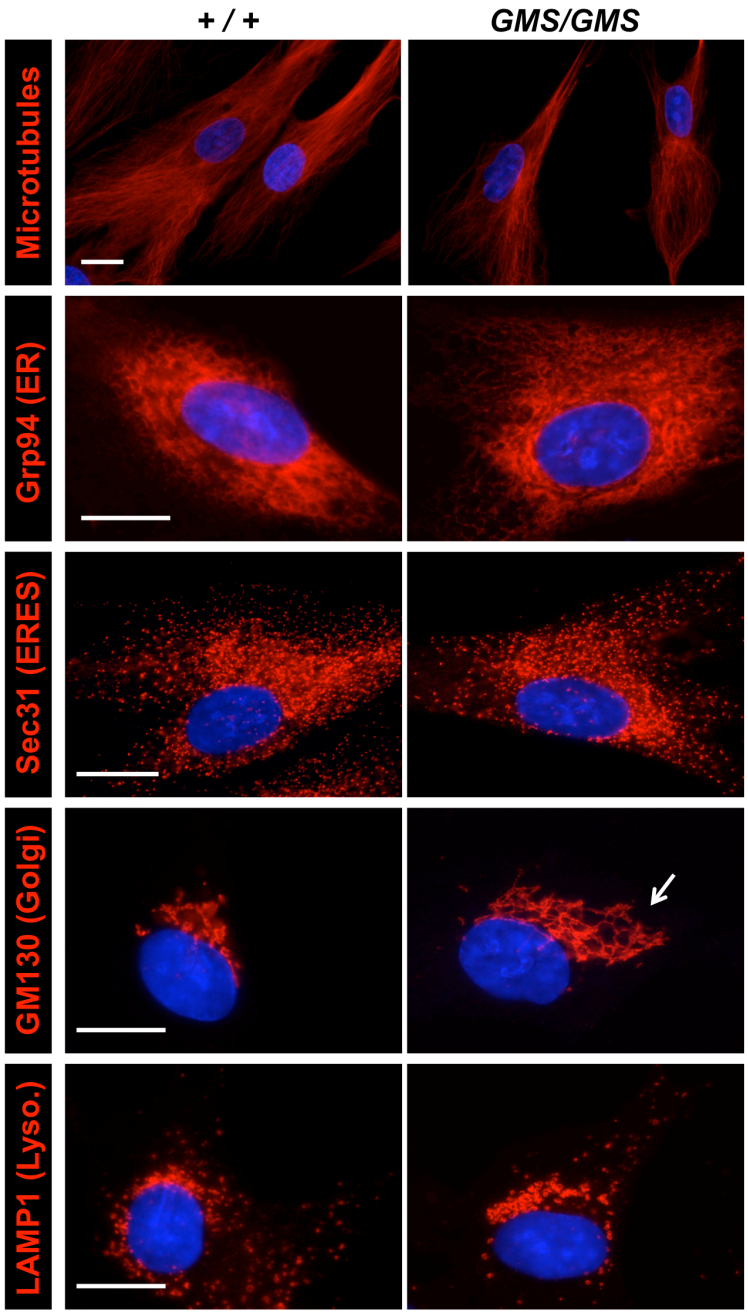

Figure S2. Amish GMS patient fibroblasts have an enlarged *cis*-Golgi compartment in a predominantly organized cytoplasm.
Wild type (+/+) or GMS patient (*GMS*/*GMS*) fibroblasts were fixed and stained with antibodies to visualize microtubules, the endoplasmic reticulum (ER), ER exit sites (ERES), the *cis*-Golgi, or lysosomes (each in red). DAPI-stained nuclei are shown in blue. Scale bars = 10µm. The arrow indicates a larger-than-normal Golgi.

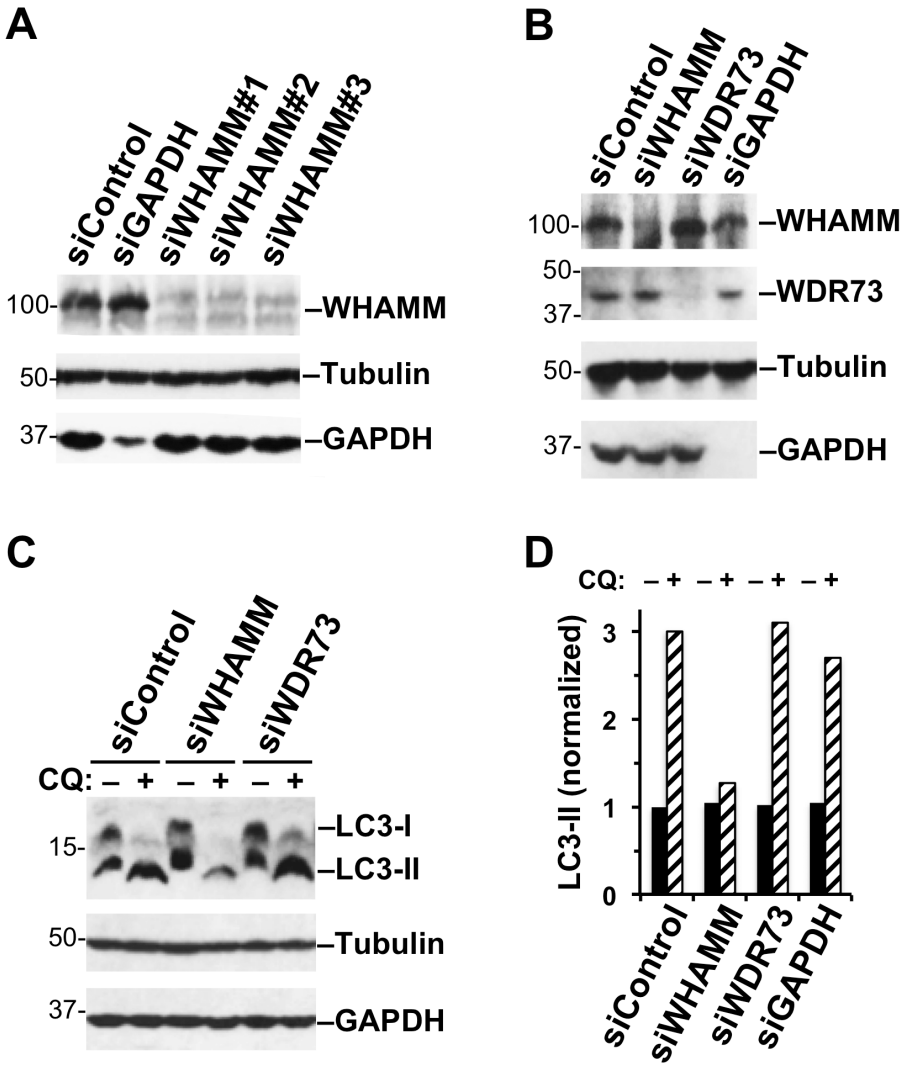

Figure S3. HeLa cells depleted of WHAMM exhibit less LC3 conversion.
A. HeLa cells were treated with control, GAPDH, or 3 independent WHAMM siRNAs and tested for protein knockdown by immunoblotting for WHAMM, Tubulin, and GAPDH. **B.** HeLa cells were treated with a control, 3 WHAMM, 3 WDR73, or a GAPDH siRNA and analyzed by immunoblotting for WHAMM, WDR73, Tubulin, and GAPDH. **C.** HeLa cells treated with siRNAs were grown in rich media (CQ –) or were starved for 90 min and treated with chloroquine (CQ +) prior to immunoblotting for LC3B, Tubulin, and GAPDH. The positions of the non-lipidated (LC3-I) and lipidated (LC3-II) forms of LC3B are indicated. **D.** The amount of LC3B in its mature LC3-II form was quantified by measuring band intensities on a representative immunoblot. Protein content in each lane was normalized to Tubulin staining, and the relative levels of LC3-II were calculated.

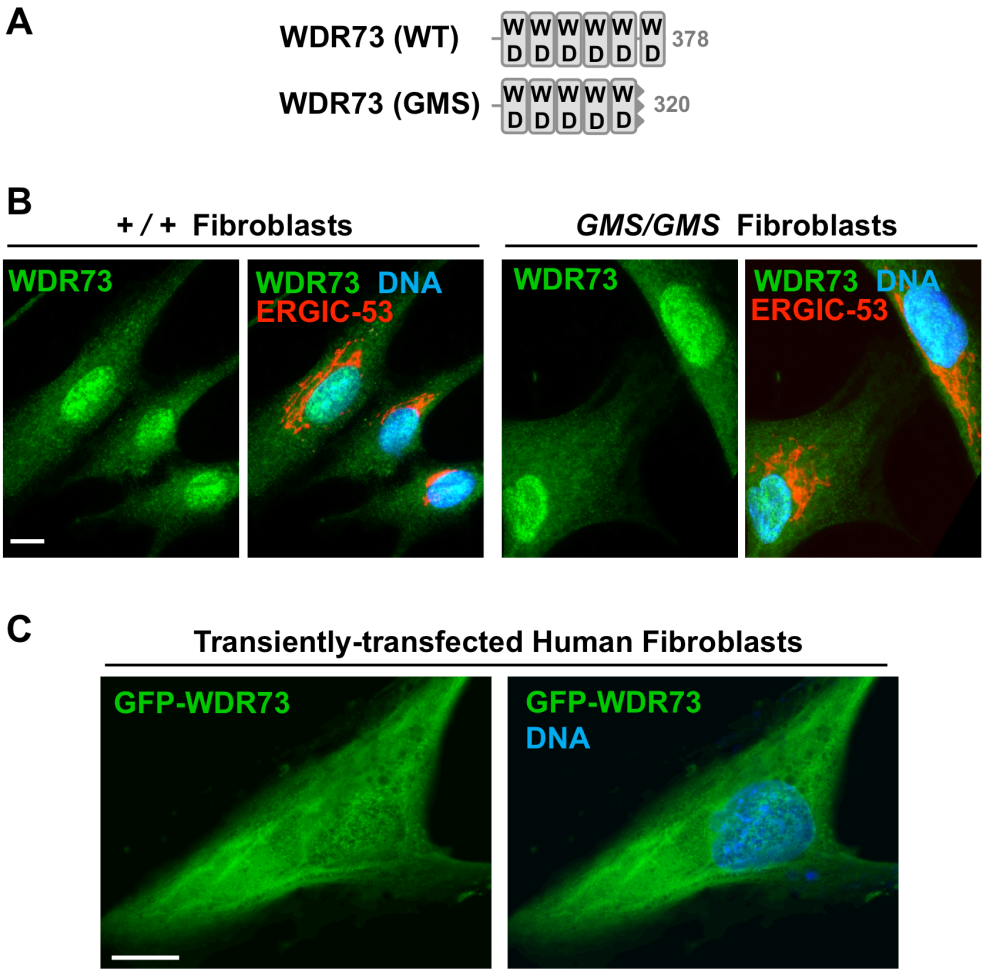

Figure S4. WDR73 exhibits a nucleo-cytoplasmic localization in interphase cells.
A. The 378-residue WDR73(WT) protein and 320-residue truncated Amish GMS variant (Jinks et al., 2015) are diagrammed.
B. Wild type (+/+) or Amish GMS patient (*GMS*/*GMS*) fibroblasts were fixed and stained with antibodies to detect WDR73 (green) or ERGIC-53 (red) and with DAPI to label DNA (blue). A nucleo-cytoplasmic localization of WDR73 was detected in both cell lines. Similar results were observed using two different commercially-available WDR73 antibodies. Scale bar = 10µm.
C. Normal fibroblasts were transfected with a plasmid encoding GFP-WDR73(WT), fixed, and stained with DAPI to label DNA (blue). GFP-WDR73 exhibited a diffuse nucleo-cytoplasmic localization. Scale bar = 10µm.

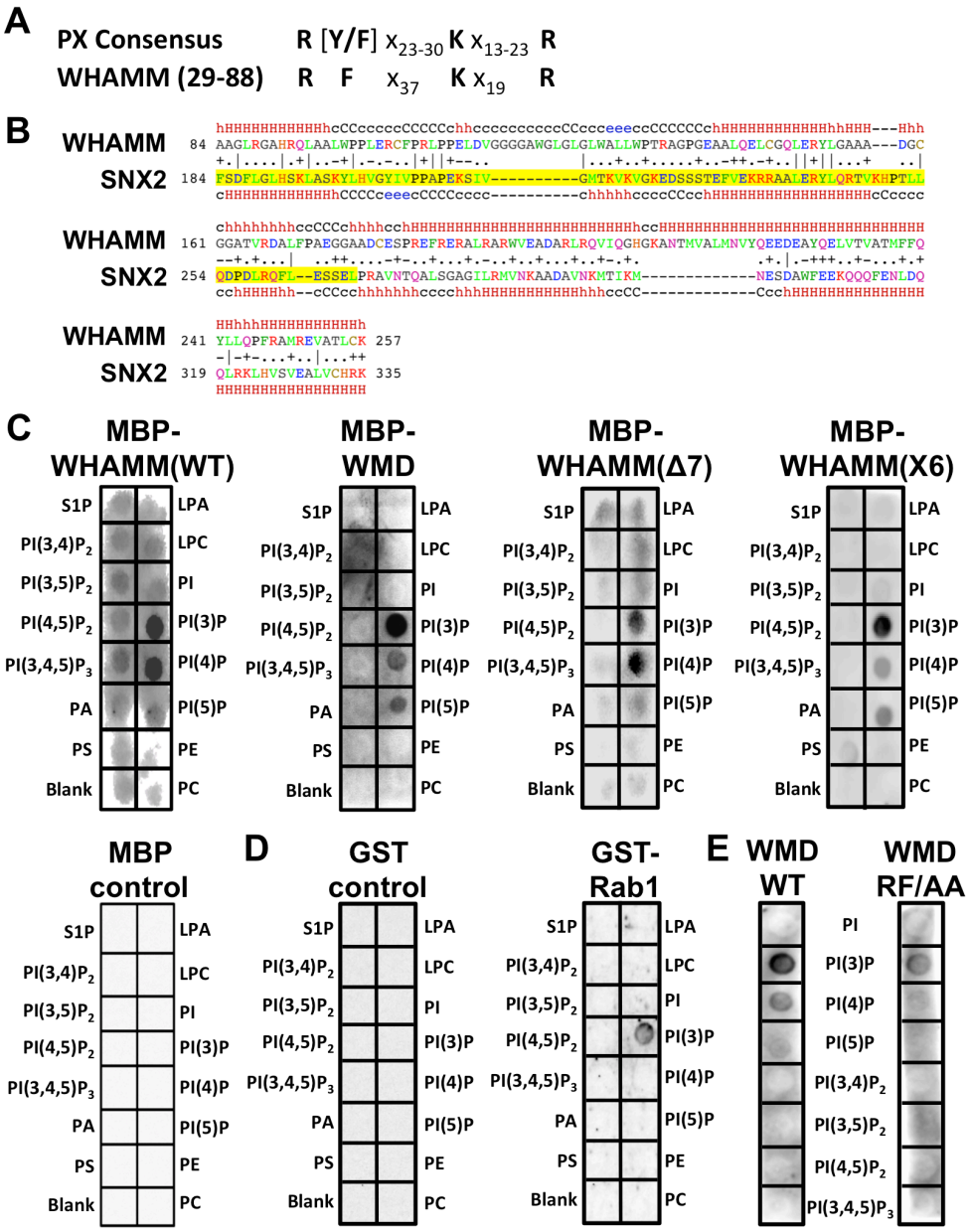

Figure S5. WMD-containing WHAMM derivatives and the small G-protein Rab1 bind to PI(3)P *in vitro*.

A. A consensus PI(3)P-binding motif from PX domains (Teasdale and Collins, 2012) is shown in comparison to residues 29-88 of WHAMM.

B. An hhpred (Soding et al., 2005) alignment of WHAMM residues 84-257 and SNX2 residues 184-335 are shown. Regions of helix (h,H) and coil (c,C) are indicated. The C-terminal portion of the PX domain of SNX2 is highlighted in yellow. WHAMM also exhibited homology to at least 6 other SNX proteins.

C-E. Different phospholipids (100 pmol each) immobilized on nitrocellulose membranes were probed with purified MBP-WHAMM(WT), MBP-WMD, MBP-WHAMM(Δ7), MBP-WHAMM(X6), MBP, GST, GST-Rab1A, MBP-WMD(WT), or MBP-WMD(RF/AA). Bound protein was detected using antibodies to MBP or GST and visualized by chemiluminescence.

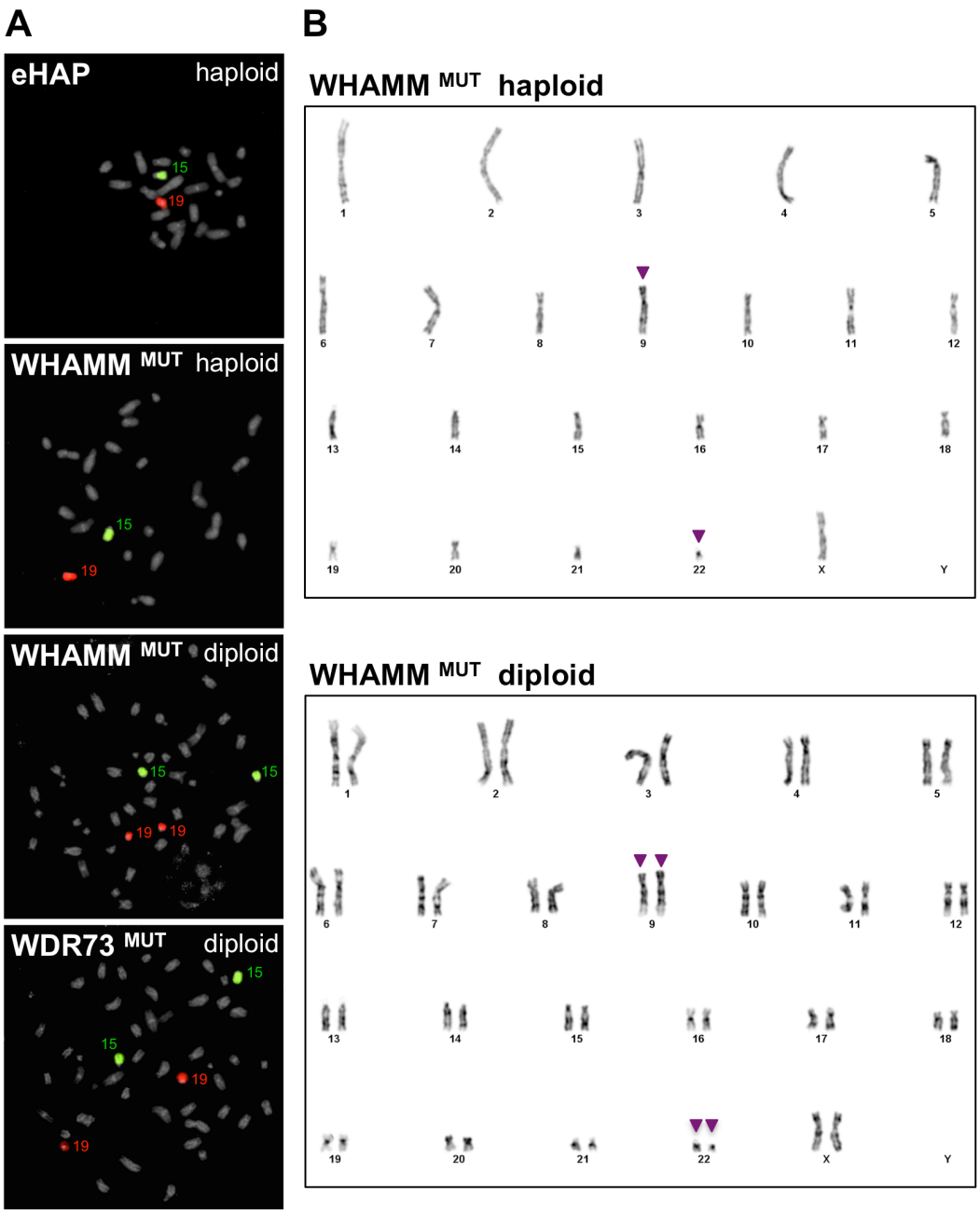

Figure S6. CRISPR-engineered cell lines have the expected karyotypes.
A. DAPI-stained chromosome spreads were treated with fluorescence *in situ* hybridization (FISH) probes for Chromosome 15 (green) and Chromosome 19 (red) to confirm that all cell lines were derived from a fully-haploid eHAP clone (Essletzbichler et al., 2014) and not the nearly-haploid HAP1 line (Carette et al., 2011). Nevertheless, eHAP, WHAMM^{MUT}, and WDR73^{MUT} cell lines each revert to autozygous diploidy over time. Representative examples of haploid and diploid spreads are shown. All spreads for eHAP, WHAMM^{MUT}, and WDR73^{MUT} contained normal copies of Chromosomes 15 and 19, irrespective of haploidy or diploidy.
B. Representative karyograms of G-banded WHAMM^{MUT} cells are shown with the expected translocation between chromosomes 9 and 22 (purple arrows) in both haploid and diploid cells. The t(9;22) was also observed with eHAP and WDR73^{MUT} cells irrespective of ploidy.